



# Fe(II)–Fe(III)-Bearing Phases As a Mineralogical Control on the Heterogeneity of Arsenic in Southeast Asian Groundwater

André Burnol, Laurent Charlet

## ► To cite this version:

André Burnol, Laurent Charlet. Fe(II)–Fe(III)-Bearing Phases As a Mineralogical Control on the Heterogeneity of Arsenic in Southeast Asian Groundwater. *Environmental Science & Technology*, American Chemical Society, 2010, 44 (19), pp.7541-7547. <10.1021/es100280h>. <hal-00521988>

**HAL Id: hal-00521988**

**<https://hal-brgm.archives-ouvertes.fr/hal-00521988>**

Submitted on 7 Aug 2015

**HAL** is a multi-disciplinary open access archive for the deposit and dissemination of scientific research documents, whether they are published or not. The documents may come from teaching and research institutions in France or abroad, or from public or private research centers.

L'archive ouverte pluridisciplinaire **HAL**, est destinée au dépôt et à la diffusion de documents scientifiques de niveau recherche, publiés ou non, émanant des établissements d'enseignement et de recherche français ou étrangers, des laboratoires publics ou privés.

1  
2  
3  
4  
5  
6  
7  
8  
9  
10  
11  
12  
13  
14  
15  
16  
17  
18  
19  
20  
21  
22  
23  
24  
25  
26  
27  
28  
29  
30  
31  
32  
33  
34  
35  
36  
37  
38  
39  
40  
41  
42  
43  
44  
45  
46  
47  
48  
49  
50  
51  
52  
53  
54  
55  
56  
57  
58  
59  
60

# Fe(II)-Fe(III)-bearing Phases as a Mineralogical Control on the Heterogeneity of Arsenic in Southeast Asian Groundwater

*ANDRE BURNOL* <sup>§‡\*</sup>, *LAURENT CHARLET* <sup>§</sup>

<sup>§</sup>LGIT-OSUG, University of Grenoble-I, BP 53, F-38041 Grenoble Cedex 9, France.

<sup>‡</sup> BRGM, Bureau de Recherches Géologiques et Minières, Environment and Process Division, 3, avenue Claude Guillemin, BP 36009, 45060 Orléans

Cedex 2, France

In preparation for **Environmental Science & Technology**

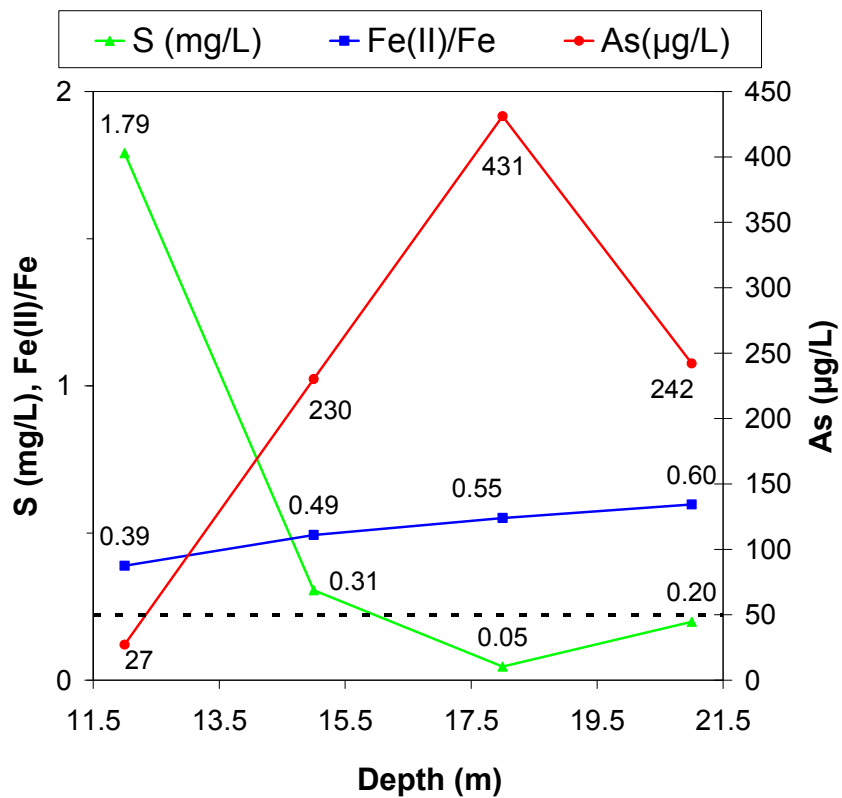
\*Corresponding author

Phone: +33 238 644 647; fax: +33 238 643 062; e-mail address: a.burnol@brgm.fr

**Abstract** (word limit: 150-200 words) (192 words)

Although groundwater arsenic constitutes a major hazard to the health of the people of Southeast Asia, the exact mineralogical origin of the arsenic in these fluvial aquifers is still under debate. Fe(III) oxides are the dominant hosts of mobilizable arsenic in the sediments, with the role of secondary Fe(II)-bearing phases like mackinawite, siderite, vivianite, magnetite and carbonate green rust (fougerite) still unclear. Based on published field data from Chakdaha (India), the importance of the phases for arsenic mobility is evaluated quantitatively using models of growing complexity. Arsenic heterogeneity can be explained by the presence of two contrasted redox zones in the aquifers, with Fe(III) oxides being the dominant sorbent for arsenic in the less reduced zones and Fe(II) sulfides and/or Fe(II) carbonates being the solid-phase hosts for arsenic under more reduced conditions below impermeable soils or close to rivers where sulfate is reduced. A 1D reactive transport model which simulates the transition between the two environments has been developed and compared to field data. The results show that microbial sulfate reduction followed by abiotic and/or biotic reduction of As(III)-bearing iron oxides accounts for the spatial heterogeneity of arsenic in such reduced aquifers.

## TOC Art



(less than 7000 words) (4480 words with references, 2 Tables, 4 Figures)

## **Introduction** (2 double spaced pages with <20 references)

The spatial heterogeneity of arsenic in shallow groundwater is well documented in many fluvial regions of Southeast Asia and occurs on very small scales with high arsenic concentrations (>100 µg/L) commonly being found within tens of meters of low concentrations, i.e. below 50 µg/L, the drinking water standard in those areas. It reflects local heterogeneities in the water recharge, water chemistry and sediment properties inherent to a young depositional floodplain environment.

The most widely accepted mechanism causing high aqueous arsenic concentrations in Southeast Asian aquifers is the microbial reductive dissolution of iron (hydr)oxides and the concomitant release of arsenic (*1*). The origin of the organic matter that drives such aquifers toward reducing conditions is, however, still under debate. Moreover, there is an observed decoupling of iron and arsenic release in both the laboratory (*2-4*) and the field (*1*). This poor As-Fe correlation could be explained by various scenarios, such as (i) a biotic reduction of As(V) to As(III) which sorbs more weakly onto iron oxyhydroxides (*4*), (ii) a precipitation of different secondary Fe(II) phases after the reductive dissolution of Fe(III) phases (*5*), (iii) a weaker sorption of arsenic by the secondary Fe(II) phases (*6*) and references therein).

The combination of local hydrology and geochemistry in those aquifers results in two contrasted geochemical environments: a moderately reduced environment characterized by low Fe(II)/Fe ratios with relatively high sulfate and low arsenic concentrations (<50 µg/L As), and a more reduced (hereafter termed “anoxic”) environment characterized by higher Fe(II)/Fe ratios with lower sulfate and higher As concentrations. These two environments have been observed along the Mekong River in Cambodia (*7-9*), along the Red River in Vietnam (*10*), along a stream at the K site in Araihasar, Bangladesh (*11, 12*) and along the Hooghly River in Chakdaha, India (*13, 14*) (Figures 2SI and 3SI).

1  
2  
3  
4  
5 In these anoxic environments, arsenic mobility would be controlled by the nature and distribution of  
6 secondary Fe(II) or mixed Fe(II)/Fe(III) phases like mackinawite Fe(II)S, magnetite Fe(II)Fe(III)<sub>2</sub>O<sub>4</sub>,  
7 fougurite Fe(II)<sub>4</sub>Fe(III)<sub>2</sub>(OH)<sub>12</sub>CO<sub>3</sub>·2H<sub>2</sub>O (the mineral analogue of carbonate green rust), siderite  
8 Fe(II)CO<sub>3</sub> and vivianite Fe(II)<sub>3</sub>(PO<sub>4</sub>)<sub>2</sub>·8H<sub>2</sub>O (15-17).

9  
10  
11  
12  
13  
14 The aim of the present paper is to infer from Chakdaha data (India) different scenarios of arsenic  
15 release using models of growing complexity like Kd sorption, surface complexation and 1D reactive  
16 transport models.  
17  
18  
19  
20  
21  
22

## 23 **Models**

24  
25  
26 **Iron(III) surface complexation model.** Geochemical speciation and sorption were performed with  
27 PHREEQC version 2.15 (18) using the WATEQ4F database (19). The protonation constants of  
28 arsenite, being consistent with the sorption data calculated by Dixit and Hering (20), were extracted  
29 from the MINEQL V4.5 database (21). Only arsenite is considered because arsenate reduction is  
30 expected to precede crystallised iron (e.g. goethite, hematite) and sulphate reduction on a  
31 thermodynamic basis (9). The interaction between arsenite and iron(III) surface is described by the  
32 two-layer surface complexation model from Dzombak and Morel (22) with only one type of  
33 adsorption site being considered, i.e. the weak sites ≡(w)FeOH (Table 1). Campbell et al. (23)  
34 estimated that the maximum surface site density for arsenic onto ferric hydroxides is [≡(w)FeOH] =  
35 0.117 Fe<sub>T</sub> with Fe<sub>T</sub> the total solid Fe concentration. The amount of extractable iron in the sediments  
36 ranged from 1.6 to 9.7 wt.% at the Chakdaha site (14) but only a fraction of this iron is contained in  
37 mineral phases with available surface sites for arsenic. This available fraction, which includes  
38 amorphous phases (e.g. ferrihydrite) and also more crystalline Fe minerals (e.g. hematite, goethite),  
39 can be approximated by the reducible iron pool of the sediment, typically 10 to 20% of the solid phase  
40 iron, as opposed to the recalcitrant fraction (e.g. Fe incorporated in silicate minerals) (24). The  
41  
42  
43  
44  
45  
46  
47  
48  
49  
50  
51  
52  
53  
54  
55  
56  
57  
58  
59  
60

1  
2  
3  
4  
5 reducible Fe fraction in our model is assumed to be 20 % of the total iron, i.e. 0.2 wt.% supposing 1  
6  
7 wt.% of iron in sediment.  
8

9  
10 **1D generic reactive transport model.** Coupling the geochemical reactions with a constant 1D  
11  
12 advective flow was performed with PHREEQC version 2.15 (18) using the WATEQ4F database (19).  
13  
14 A high pore velocity of 5 cm/day (see SI), i.e.  $5.8 \cdot 10^{-7}$  m/s, is selected for simulating a generic 1D  
15  
16 flow path from an area recharge to a depth range (e.g. the Wells I3-5-6-7).  
17  
18

19 The model's reaction processes at local equilibrium are aqueous speciation, surface complexation  
20  
21 onto iron oxide (Table 1) and mineral dissolution/precipitation. Microbially mediated terminal  
22  
23 electron accepting processes (TEAPs) are included in the model under kinetic constraints. A first  
24  
25 order dependency for surface-complexed sulfide concentrations with respect to the abiotic reduction  
26  
27 of iron could be considered (Table 2). The sorption of arsenic onto secondary phases (siderite or  
28  
29 mackinawite) is included in the model using the  $K_d$  at pH 7 (Table 1) and a very high kinetics (Table  
30  
31 2, SI). The Michaelis-Menten and Monod kinetic approaches are traditionally used for modeling  
32  
33 TEAPs coupled with transport (25). A well-known shortcoming of this approach is that it does not  
34  
35 account for the complete competitive exclusion or/and the thermodynamic feasibility of these TEAPs  
36  
37 (26, 27). In this generic study, the total rate of organic carbon oxidation ( $R_c$ ) is determined  
38  
39 independently from the concentration of species other than organic carbon.  $R_c$  is assumed to be  
40  
41 representative of the average reactivity of the sedimentary organic carbon over the vertical range of  
42  
43 interest and is broken down into the contributions of individual metabolic pathways represented by  
44  
45 nitrate, sulfate and/or iron reduction (see SI). The sequential use of terminal electron acceptors based  
46  
47 on differences in their redox potential can be simulated by defining critical concentrations of electron  
48  
49 acceptors below which the model shifts to the next available electron acceptor. The limiting  
50  
51 concentrations for  $\text{NO}_3^-$ ,  $\text{SO}_4^-$ , Fe(III) and the initial concentrations are fitted values obtained by  
52  
53 using data of Wells I3-5-6-7 (Tables 2 and 1SI).  
54  
55  
56  
57  
58  
59  
60

The favorability of sulfate reduction could exceed the favorability of crystallized iron, e.g. goethite or hematite, at commonly observed  $Fe^{2+}$  concentrations in the Bengali aquifers (9). In the scenario (a), it is supposed that nitrate, sulfate, and iron reduction are successive external electron acceptors, but without considering the abiotic reduction of Fe(III) by  $HS^-$ . Conversely, in scenario (b), the abiotic reduction of iron by  $HS^-$  is considered, but without considering dissimilatory iron reduction. Comparing the results of both scenarios will determine which respiration process could account for the release of arsenic.

**Iron(II) Kd sorption model.** Iron and arsenic total concentrations, respectively  $As_T$  and  $Fe_T$ , are assumed to be conserved between the two redox contrasted environments (see SI). The conservation between the two closed systems is described by the two following equations:

$$As_T = [As]_{\max} \times (1 + \sum_i M_i \times K_d^i) \quad (1)$$

$$Fe_T = \sum_i M_i \times f_i \quad (2)$$

where  $[As]_{\max}$  is a high aqueous concentration of As(III) in the anoxic environment (e.g.  $5 \mu\text{mol/L}$ ),  $M_i$  the mass of the  $i$ -th Fe(II)-bearing phase (mackinawite, vivianite, magnetite, fougurite, siderite),  $K_d^i$  the adsorption/partition coefficient for As(III) onto the  $i$ -th phase, and  $f_i$  the percentage of iron in the total weight of the  $i$ -th phase. Calculation of the  $K_d^i$  coefficients shows that, except for vivianite,  $K_d^i$  depends strongly on pH, in particular between pH 7 and 7.5 which is the variation range at the Chakdaha site (28). The  $K_d^i$  coefficients are calculated from the adsorbed As fraction called  $s$  and the  $i$ -th solid concentration called  $d^i$  (g/L) obtained from the sorption isotherms published in the literature (see Tables 1 and 3SI):

$$K_d^i = \frac{s}{(1-s) \times d^i} \quad (3)$$

MATLAB® (R2006b, The MathWorks, Natick, MA) is used to solve the problem in cases with two, three or four sorbents. In every case, there are only two unknowns in eq 1 and in eq 2.



## Results and Discussion

**Field site.** A transect of simultaneously collected groundwater and aquifer solids perpendicular to the banks of the Hooghly River in Chakdaha (West Bengal, India) was used to calibrate the different models (Figures 1 and 1SI). The methods of sample collection with the needle-sampler and chemical analysis are described by van Geen et al. (29) and a description of the analytical methods is given in SI.

**Two contrasted redox environments in Chakdaha subsurface.** Two contrasted redox environments are distinguished in Chakdaha subsurface (13): fairly permeable sandy soils (indicated by low electromagnetic conductivity) where moderately reduced conditions prevail with low Fe(II)/Fe solid ratios ( $<0.5$ ), underlain by more impermeable clayey soils (indicated by high electromagnetic conductivity) where more reduced conditions prevail with high Fe(II)/Fe solid ratios ( $>0.5$ ). The sandy soils are also characterized by high permeability, a high concentration of sulfate ions ( $>1$  mg/L S), and a low arsenic concentration ( $<50$   $\mu\text{g/L}$  As), whereas the underlying clayey soils are characterized by low permeability, a low sulfate concentration ( $<1$  mg/L S), and a high arsenic concentration ( $>100$   $\mu\text{g/L}$  As). This contrast is particularly observed in I7 Well, with a negative correlation ( $-0.85$ ) between aqueous arsenic and sulfate and a positive correlation ( $+0.9$ ) between aqueous arsenic and solid Fe(II)/Fe ratio. The low Fe(II)/Fe ratio is attributed to iron-oxide coatings on quartz and mica sand particles, while the high Fe(II)/Fe solid ratio may be related to Fe(II)-rich minerals like Acid Volatile Sulfides (AVS; e.g. disordered mackinawite), as well as fine vivianite, siderite, fougurite and magnetite particles. These contrasted solid and aqueous environments play likely a role in the release of arsenic: the Fe(III) oxide vs. Fe(II) sulfide/carbonate solid phases correspond to high S(VI) vs. high As(III) aqueous phases.

1  
2  
3  
4  
5 In order to test different scenarios, geochemical computations were performed on two closed model  
6 systems; namely a Fe(III) oxide-As(III)-SO<sub>4</sub>-water system known as the “Iron(III) surface  
7 complexation model” and a Fe(II) sulfide/carbonate-As(III)-H<sub>2</sub>S-water system known as the “Iron(II)  
8 Kd sorption model”. In the moderately reduced environment, solid iron is assumed to be the unique  
9 sorbent and arsenite the unique sorbate. In the anoxic environment, the Fe(II)-bearing phases  
10 (magnetite, siderite, fougurite, vivianite) are potential sorbents and As(III) the unique sorbate. A “1D  
11 generic reactive transport model” is developed to simulate the transition between these two  
12 environments.  
13  
14  
15  
16  
17  
18  
19  
20  
21  
22

23 **Iron(III) surface complexation model.** A typical low concentration of arsenic is set to 17 µg/L  
24 (Table 1SI) and the pH to 7, the mean pH at Chakdaha site (14). The sorption equilibrium calculated  
25 by PHREEQC results in a total of 0.76 mmol sorbed As(III) L<sup>-1</sup> as the sum of ≡(w)FeHAsO<sub>3</sub><sup>-</sup> and  
26 ≡(w)FeH<sub>2</sub>AsO<sub>3</sub> (Table 2SI). Assuming a porosity of 0.25 and a density of 2.62, it corresponds to a  
27 sorbed arsenic concentration of 7.3 mg kg<sup>-1</sup>. The sediment extraction by phosphates dislodges by  
28 anion exchange the relatively mobile fraction of As bound to Fe oxhydroxides and, potentially, As  
29 bound to adsorbed humic acids. This fraction within the Chakdaha sediments ranged from 0.5 to 9 mg  
30 kg<sup>-1</sup> in Wells I3-5-6-7 (mean value 2.34 mg kg<sup>-1</sup>) (13). This surface model result is therefore  
31 consistent with the P-extractable arsenic data.  
32  
33  
34  
35  
36  
37  
38  
39  
40  
41  
42  
43

44 **1D generic reactive transport model.** The processes monitored in the above closed system are  
45 obviously not representative of those occurring in anoxic conditions: the release of arsenic depends  
46 not only on sorption interactions at local equilibrium but also on coupled reactive transport under  
47 kinetic constraints for redox sensitive elements like As, N, S, Fe. A reactive transport model was  
48 therefore developed in order to simulate a 1D flow path between the two contrasted redox systems.  
49 The calculation scheme results in smooth transitions between spatial redox zones as commonly  
50 observed *in situ* (30). The oxidation rate of carbon C(0) is assumed to be constant along the 1D path  
51  
52  
53  
54  
55  
56  
57  
58  
59  
60

1  
2  
3  
4  
5 for nitrate and sulfate (see Model section). This oxidation rate is fixed to a maximum value of 2 mM  
6  
7 year<sup>-1</sup> consistent with the observed range of 1.0-1.5 mM year<sup>-1</sup> for sulfate reduction found by  
8  
9 Jakobsen et al. (31). Assuming a constant carbon oxidation rate in scenario (a), the iron reduction rate  
10  
11 would be 8 mM Fe year<sup>-1</sup> (one e<sup>-</sup> consumed instead of 8 e<sup>-</sup>). This “high” iron bioreduction rate is  
12  
13 consistent with our previous batch experiments with amorphous 2-line ferrihydrite (4) but the iron  
14  
15 reduction rate for crystallized iron, e.g. goethite, is very likely below the value for the amorphous  
16  
17 phase like 2-line ferrihydrite (32). A “low” rate of 1.5 mM Fe year<sup>-1</sup> was indeed fitted in scenario (a)  
18  
19 using Well I7 (Figure 2).  
20  
21  
22

23  
24 The first result of (a) is that the maximum simulated concentration of As is in the range of the  
25  
26 observed high arsenic concentrations (between 200 and 500 µg/L). A sensitivity analysis to pore  
27  
28 velocity and to the Fe(III) reduction rate illustrates however that the maximum release of arsenic  
29  
30 depends on the balance between the flow velocity and the chemical kinetics: a “low” flow velocity or  
31  
32 a “high” Fe(III) reduction rate will both correspond to a dissolved arsenic peak slightly above 1 mg/L  
33  
34 (Figure 4SI). Considering the uncertainty on both parameters at the Chakdaha site, the timescales the  
35  
36 model fits are therefore probably not significant.  
37  
38

39  
40 In scenario (a), the spatial profiles of the redox sensitive elements, i.e. the decrease of NO<sub>3</sub><sup>-</sup>, SO<sub>4</sub><sup>-</sup>  
41  
42 and the increase of Fe(II) and As(III) along the 1D vertical path, are all correctly simulated (Figure 2)  
43  
44 but the increase in alkalinity is slightly overestimated. The simulated K<sub>d</sub> of arsenic onto siderite is  
45  
46 closed to the K<sub>d</sub> value at pH 7 (Table 1). The pore waters at the bottom of the profile in Wells I3-5-6-  
47  
48 7 are undersaturated with respect to calcite and near from equilibrium with respect to siderite (except  
49  
50 for I5). Combining all the samples during the period 2000-2002 showed however that the Chakdaha  
51  
52 groundwaters are generally at local equilibrium with calcite and other carbonates (e.g. rhodochrosite,  
53  
54 dolomite) and oversaturated with respect to siderite (14).  
55  
56  
57  
58  
59  
60

1  
2  
3  
4  
5 In scenario (b), the aqueous As and solid Fe(2)/Fe are not consistent with the data (Figure 3). The  
6 comparison of both scenarios demonstrates that sulfate-reducing bacteria (SRB) activity alone is not  
7 sufficient and that iron-reducing bacteria (IRB) activity is needed to explain the release of arsenic in  
8 these Wells. The comparison shows also that the simulated chemical zones are quite different: (a)  
9 shows a transition between the sulfidic and ferruginous zones; in (b), HS<sup>-</sup> reduces solid Fe(III) and  
10 thus does not accumulate despite active sulfate reduction, whilst producing Fe(II) precipitates as  
11 siderite in the sulfate reduction zone. Sulfides were not measured during this campaign but there was  
12 no significant smelling during the sampling and a sulfidic zone is therefore unlikely. Moreover, a  
13 sediment vertical profile in Cambodia revealed siderite in a deep reduced zone that is not preceded by  
14 a sulfidic zone (9). Finally, it shows that a more appropriate scenario could be the combining of both  
15 scenarios (see SI and Figure 5SI).

16  
17  
18  
19  
20  
21  
22  
23  
24  
25  
26  
27  
28  
29  
30  
31 In the last scenario, termed (c), a concurrent dissimilatory reduction of iron and sulfate as already  
32 observed in field studies (30) or at micro-scale (33) is tested (see SI). In that case, the precipitation of  
33 FeS(s) removes HS<sup>-</sup> and Fe<sup>2+</sup> and therefore increases the favorability of both reducers (IRB and SRB)  
34 by increasing the energy gain. The arsenic aqueous profile in (c) is consistent with the data (Figure 3).  
35 Therefore, a concurrent bacterial respiration process between IRB and SRB can not be excluded.

36  
37  
38  
39  
40  
41  
42 **Alternative biogeochemical mechanisms omitted in 1D model.** Other (bio)geochemical  
43 processes may consume carbonates and are not considered in this simplified model like the  
44 methanogenesis or/and the rhodochrosite precipitation (14). Moreover, our approach clearly shortcuts  
45 the multiple steps of the complex organic matter breakdown: the kinetic rate of carbon oxidation is  
46 assumed to be constant. The past decade has seen a large number of models that couple the kinetic  
47 expressions with the thermodynamic constraints, either in the fermentation step or in the terminal  
48 electron accepting reaction step. One of the most used representations is the so-called “partial redox  
49 disequilibrium” model, first developed by McNab and Narasimhan (34). The idea is to separate  
50  
51  
52  
53  
54  
55  
56  
57  
58  
59  
60

1  
2  
3  
4  
5 organic matter degradation into only two steps. The first step comprises hydrolyzation and  
6 fermentation, producing labile organic carbon, nutrients and inorganic carbon  $\text{HCO}_3^-$ ; the produced  
7 number of inorganic moles per mole of labile organic carbon is generally unknown. The key point is  
8 that this first step limits the overall rate and that the second step is the terminal electron reactions step,  
9 which is faster and close to equilibrium.  
10  
11  
12  
13  
14  
15

16 **Iron(II) Kd sorption model in Southeast Asian aquifers: a sensitivity analysis.** The  
17 concentration of solid As ranges between 2 and 22  $\text{mg kg}^{-1}$  (14). A typical sediment with about 1  
18 wt.% of Fe-oxides and about 2  $\text{mg kg}^{-1}$  of solid As is considered (see SI). The one-phase systems  
19 (with a unique sorbent for arsenite) and the multiple-phase systems (with different sorbents) have  
20 been systematically investigated (Table 4SI).  
21  
22  
23  
24  
25  
26  
27

28 In the one-phase systems, an abundance of around 15 wt.% Fe in mackinawite is needed. This result  
29 is much higher than the observed values of AVS in Araihasar (Bangladesh), where AVS varies from  
30 0.2 to 2  $\mu\text{mol g}^{-1}$  sediment (J. Métral, personal communication); AVS represents only 0.11 to 1.1  
31 wt.% iron assuming about 1 wt.% iron in the sediment.  
32  
33  
34  
35  
36

37 Using Kd at pH 7 and 7.5, a similar calculation shows that between 56 wt.% and 84 wt.% iron in  
38 siderite is needed, assuming that siderite is the dominant host for arsenite. This result is a little higher  
39 than observed ratios of between 35% and 40% found in Cambodian sediments (9). The groundwater  
40 in the shallow reducing aquifers is strongly supersaturated for both vivianite  $\text{Fe(II)}_3(\text{PO}_4)_2 \cdot 8\text{H}_2\text{O}$  and  
41 hydroxyapatite  $\text{Ca}_5(\text{PO}_4)_3\text{OH}$  in Bangladesh (24) and also supersaturated for vivianite in Vietnam  
42 (35). The highest concentration of P derived from sandy horizons of the Bengal basin was reported to  
43 be equal to 214  $\text{mg P/kg}$  (36). Assuming that vivianite is the dominant Fe-bearing host of sedimentary  
44 phosphorus, then vivianite represents only around 6 wt.% Fe (see SI). Conversely, if we assume that  
45 vivianite is the unique sorbent for arsenite, then 87 wt.% of iron in vivianite is needed. The  
46 conclusion is that vivianite, mackinawite and magnetite are likely not the dominant host for arsenite at  
47  
48  
49  
50  
51  
52  
53  
54  
55  
56  
57  
58  
59  
60

1  
2  
3  
4  
5 pH 7 and that siderite is the better candidate as the main sorbent (at least in the short list investigated  
6  
7 in this work).  
8

9  
10 In multiple-phase systems, the residual iron is assumed to be distributed within two, three or four  
11 Fe(II)-bearing phases: if mackinawite represents 1 wt.% of the solid iron and if furthermore the  
12 dominant hosts of arsenite are siderite and magnetite, then an abundance of 74 wt.% siderite and 25  
13 wt.% magnetite are needed at pH 7 (see SI). Two possible four-phase systems are shown in Figure 4  
14  
15 with a similar calculated Fe(II)/Fe ratio (0.83 with magnetite or 0.9 with fougurite). The main  
16  
17 conclusion for one-phase systems is still valid with multiple-phase systems: siderite seems to be the  
18  
19 better candidate as the dominant host for arsenite at pH 7.  
20  
21  
22  
23  
24  
25

26 **Implication for arsenic heterogeneity in reducing aquifers.** We first demonstrate that low  
27 concentrations of arsenic in moderately reduced zones at the Chakdaha site could be explained by a  
28 adsorption of As(III) onto solid Fe(III) oxides. We then hypothesize that the observed high  
29 concentrations of arsenic in the anoxic zones could be quantitatively interpreted by a reduction of  
30 solid Fe(III) oxides followed by sorption of As(III) on different Fe(II)-bearing phases: while Fe(II)  
31 sulfide (e.g. disordered mackinawite) or vivianite are not the dominant host for arsenite, the ferrous  
32 carbonates (like siderite or/and fougurite) very likely play a major role in such reduced systems. We  
33 finally simulate the transition between the two contrasted redox zones and compare different  
34 energetically possible scenarios of arsenic release. This comparison shows that the reduction of solid  
35 iron by biogenic sulfides is not sufficient to explain this release. The reactive transport model shows  
36 also that both scenarios, assuming a successive or a concomitant sulfate and iron reduction, are  
37 consistent with the observations at Chakdaha site.  
38  
39  
40  
41  
42  
43  
44  
45  
46  
47  
48  
49  
50  
51  
52  
53  
54  
55  
56  
57  
58  
59  
60

## Acknowledgments

The authors gratefully acknowledge RGNDWM, Govt. of India, IFCPAR and CNRS (EC2CO Programme) for giving financial support. One of the authors (AB) is thankful to the Bureau de Recherches Géologiques et Minières (BRGM) for supporting this publication work and to Nolwenn Croiset for helpful discussions about Phreeqc modeling.

## Supporting Information Available

This information is available free of charge via the internet at <http://pubs.acs.org/>.

## References

1. Nickson, R.T.; McArthur, J.M.; Ravenscroft, P.; Burgess, W.G.; Ahmed, K.M. Mechanism of arsenic release to groundwater, Bangladesh and West Bengal. *Appl. Geochem.* **2000**, *15*, 403-413.
2. Islam, F.S.; Gault, A.G.; Boothman, C.; Polya, D.A.; Charnock, J.M.; Chatterjee, D.; Lloyd, J.R. Role of metal-reducing bacteria in arsenic release from Bengal delta sediments. *Nature* **2004**, *430*, 68-71.
3. van Geen, A.; Rose, J.; Thoraj, S.; Garnier, J.M.; Zheng, Y.; Bottero, J.Y. Decoupling of As and Fe release to Bangladesh groundwater under reducing conditions. Part II: Evidence from sediment incubations. *Geochim. Cosmochim. Acta* **2004**, *68*, 3475-3486.
4. Burnol, A.; Garrido, F.; Baranger, P.; Joulain, C.; Dictor, M.; Bodenan, F.; Morin, G.; Charlet, L. Decoupling of arsenic and iron release from ferrihydrite suspension under reducing conditions: a biogeochemical model. *Geochemical Transactions* **2007**, *8*, 12.
5. Horneman, A.; van Geen, A.; Kent, D.V.; Mathe, P.E.; Zheng, Y.; Dhar, R.K.; O'Connell, S.; Hoque, M.A.; Aziz, Z.; Shamsudduha, M. Decoupling of As and Fe release to Bangladesh groundwater under reducing conditions. Part I: Evidence from sediment profiles. *Geochim. Cosmochim. Acta* **2004**, *68*, 3459-3473.
6. Charlet, L. and Polya, D.A. Arsenic in shallow, reducing groundwaters in southern Asia: an environmental health disaster. *Elements* **2006**, *2*, 91-96.
7. Polizzotto, M.L.; Kocar, B.D.; Benner, S.G.; Sampson, M.; Fendorf, S. Near-surface wetland sediments as a source of arsenic release to ground water in Asia. *Nature* **2008**, *454*, 505-508.



1  
2  
3  
4  
5 8. Kocar, B.D.; Polizzotto, M.L.; Benner, S.G.; Ying, S.C.; Ung, M.; Ouch, K.; Samreth, S.; Suy,  
6  
7 B.; Phan, K.; Sampson, M.; Fendorf, S. Integrated biogeochemical and hydrologic processes driving  
8  
9 arsenic release from shallow sediments to groundwaters of the Mekong delta. *Appl. Geochem.* **2008**,  
10  
11 23, 3059-3071.  
12

13  
14  
15 9. Kocar, B.D. and Fendorf, S. Thermodynamic Constraints on Reductive Reactions Influencing the  
16  
17 Biogeochemistry of Arsenic in Soils and Sediments. *Environ. Sci. Technol.* **2009**, 43, 4871-4877.  
18

19  
20  
21 10. Eiche, E.; Neumann, T.; Berg, M.; Weinman, B.; van Geen, A.; Norra, S.; Berner, Z.; Trang,  
22  
23 P.T.K.; Viet, P.H.; Stüben, D. Geochemical processes underlying a sharp contrast in groundwater  
24  
25 arsenic concentrations in a village on the Red River delta, Vietnam. *Appl. Geochem.* **2008**, 23, 3143-  
26  
27 3154.  
28

29  
30  
31 11. van Geen, A.; Zheng, Y.; Goodbred, S.; Horneman, A.; Aziz, Z.; Cheng, Z.; Stute, M.;  
32  
33 Mailloux, B.; Weinman, B.; Hoque, M.A.; Seddique, A.A.; Hossain, M.S.; Chowdhury, S.H.; Ahmed,  
34  
35 K.M. Flushing History as a Hydrogeological Control on the Regional Distribution of Arsenic in  
36  
37 Shallow Groundwater of the Bengal Basin. *Environ. Sci. Technol.* **2008**, 42, 2283-2288.  
38

39  
40  
41 12. Radloff, K.A.; Manning, A.R.; Mailloux, B.; Zheng, Y.; Moshir Rahman, M.; Rezaul Huq, M.;  
42  
43 Ahmed, K.M.; Geen, A.v. Considerations for conducting incubations to study the mechanisms of As  
44  
45 release in reducing groundwater aquifers. *Appl. Geochem.* **2008**, 23, 3224-3235.  
46

47  
48  
49 13. Metral, J.; Charlet, L.; Bureau, S.; Mallik, S.; Chakraborty, S.; Ahmed, K.; Rahman, M.; Cheng,  
50  
51 Z.; van Geen, A. Comparison of dissolved and particulate arsenic distributions in shallow aquifers of  
52  
53 Chakdaha, India, and Araihasar, Bangladesh. *Geochemical Transactions* **2008**, 9, 1.  
54  
55  
56  
57  
58  
59  
60

- 1  
2  
3  
4  
5 14. Nath, B.; Chakraborty, S.; Burnol, A.; Stüben, D.; Chatterjee, D.; Charlet, L. Mobility of arsenic  
6 in the sub-surface environment: An integrated hydrogeochemical study and sorption model of the  
7 sandy aquifer materials. *Journal of Hydrology* **2009**, *364*, 236-248.  
8  
9  
10  
11  
12 15. Thinnappan, V.; Merrifield, C.M.; Islam, F.S.; Polya, D.A.; Wincott, P.; Wogelius, R.A. A  
13 combined experimental study of vivianite and As (V) reactivity in the pH range 2–11. *Appl.*  
14 *Geochem.* **2008**, *23*, 3187-3204.  
15  
16  
17  
18  
19  
20 16. Jönsson, J. and Sherman, D.M. Sorption of As(III) and As(V) to siderite, green rust (fougerite)  
21 and magnetite: Implications for arsenic release in anoxic groundwaters. *Chemical Geology* **2008**, *255*,  
22 173-181.  
23  
24  
25  
26  
27  
28 17. Wolthers, M.; Charlet, L.; van Der Weijden, C.H.; van der Linde, P.R.; Rickard, D. Arsenic  
29 mobility in the ambient sulfidic environment: Sorption of arsenic(V) and arsenic(III) onto disordered  
30 mackinawite. *Geochim. Cosmochim. Acta* **2005**, *69*, 3483-3492.  
31  
32  
33  
34  
35  
36 18. Parkhurst, D.L.; Appelo, C.A.J. *User's guide to Phreeqc (version 2)- a computer program for*  
37 *speciation, batch-reaction, one-dimensional transport, and inverse geochemical calculation;*  
38 *USGS: Denver, 1999.*  
39  
40  
41  
42  
43  
44 19. Ball, J.W.; Nordstrom, D.K. *User's Manual for WATEQ4F, with Revised Thermodynamic Data*  
45 *Base and Test Cases for Calculating Speciation of Major, Trace, and Redox Elements in Natural*  
46 *Waters; USGS: Denver, 1991.*  
47  
48  
49  
50  
51 20. Dixit, S. and Hering, J.G. Comparison of arsenic(V) and arsenic(III) sorption onto iron oxide  
52 minerals: Implications for arsenic mobility. *Environ. Sci. Technol.* **2003**, *37*, 4182-4189.  
53  
54  
55  
56  
57 21. Schecher, W.D.; McAvoy, D.C. *MINEQL+, V4.5, Users Manual; Hallowell: ME, 1998.*  
58  
59  
60

1  
2  
3  
4  
5 22. Dzombak, D.A.; Morel, F.M.M. *Surface Complexation Modeling: Hydrous Ferric Oxide*; John  
6  
7 Wiley & Sons: New York, 1990.

8  
9  
10 23. Campbell, K.M.; Malasarn, D.; Saltikov, C.W.; Newman, D.K.; Hering, J.G. Simultaneous  
11  
12 Microbial Reduction of Iron(III) and Arsenic(V) in Suspensions of Hydrous Ferric Oxide. *Environ.*  
13  
14 *Sci. Technol.* **2006**, *40*, 5950-5955.

15  
16  
17 24. Swartz, C.H.; Blute, N.K.; Badruzzman, B.; Ali, A.; Brabander, D.; Jay, J.; Besancon, J.; Islam,  
18  
19 S.; Hemond, H.F.; Harvey, C.F. Mobility of arsenic in a Bangladesh aquifer: Inferences from  
20  
21 geochemical profiles, leaching data, and mineralogical characterization. *Geochim. Cosmochim. Acta*  
22  
23 **2004**, *68*, 4539-4557.

24  
25  
26 25. Hunter, K.S.; Wang, Y.; Van Cappellen, P. Kinetic modeling of microbially-driven redox  
27  
28 chemistry of subsurface environments: coupling transport, microbial metabolism and geochemistry. *J.*  
29  
30 *Hydrol. (Amst. )* **1998**, *209*, 53-80.

31  
32  
33 26. Curtis, G.P. Comparison of approaches for simulating reactive solute transport involving  
34  
35 organic degradation reactions by multiple electron acceptors. *Computers & Geosciences* **2003**, *29*,  
36  
37 319-329.

38  
39  
40 27. Heimann, A.; Jakobsen, R.; Blodau, C. Energetic Constraints on H<sub>2</sub>-Dependent Terminal  
41  
42 Electron Accepting Processes in Anoxic Environments: A Review of Observations and Model  
43  
44 Approaches. *Environ. Sci. Technol.* **2010**, *44*, 24-33.

45  
46  
47 28. Charlet, L.; Chakraborty, S.; Appelo, C.A.J.; Roman-Ross, G.; Nath, B.; Ansari, A.A.; Lanson,  
48  
49 M.; Chatterjee, D.; Mallik, S.B. Chemodynamics of an arsenic "hotspot" in a West Bengal aquifer: A  
50  
51 field and reactive transport modeling study. *Appl. Geochem.* **2007**, *22*, 1273-1292.  
52  
53  
54  
55  
56  
57  
58  
59  
60

- 1  
2  
3  
4  
5 29. van Geen, A.; Protus, T.; Cheng, Z.; Horneman, A.; Seddique, A.A.; Hoque, M.A.; Ahmed,  
6  
7 K.M. Testing Groundwater for Arsenic in Bangladesh before Installing a Well. *Environ. Sci. Technol.*  
8  
9 **2004**, *38*, 6783-6789.
- 10  
11  
12 30. Postma, D. and Jakobsen, R. Redox zonation; equilibrium constraints on the Fe(III)/SO<sub>4</sub> -  
13  
14 reduction interface. *Geochim. Cosmochim. Acta* **1996**, *60*, 3169-3175.
- 15  
16  
17 31. Jakobsen, R. and Cold, L. Geochemistry at the sulfate reduction–methanogenesis transition zone  
18  
19 in an anoxic aquifer—A partial equilibrium interpretation using 2D reactive transport modeling.  
20  
21 *Geochim. Cosmochim. Acta* **2007**, *71*, 1949-1966.
- 22  
23  
24  
25 32. Bonneville, S.; Van Cappellen, P.; Behrends, T. Microbial reduction of iron(III) oxyhydroxides:  
26  
27 effects of mineral solubility and availability. *Chem. Geol.* **2004**, *212*, 255-268.
- 28  
29  
30  
31 33. Motelica-Heino, M.; Naylor, C.; Zhang, H.; Davison, W. Simultaneous Release of Metals and  
32  
33 Sulfide in Lacustrine Sediment. *Environ. Sci. Technol.* **2003**, *37*, 4374-4381.
- 34  
35  
36 34. McNab, W.W., J. and Narasimhan, T.N. Modeling reactive transport of organic compounds in  
37  
38 groundwater using a partial redox disequilibrium approach. *Water Resour. Res.* *30*, 2619-2635.
- 39  
40  
41 35. Postma, D.; Larsen, F.; Minh Hue, N.T.; Duc, M.T.; Viet, P.H.; Nhan, P.Q.; Jessen, S. Arsenic  
42  
43 in groundwater of the Red River floodplain, Vietnam: Controlling geochemical processes and reactive  
44  
45 transport modeling. *Geochim. Cosmochim. Acta* **2007**, *71*, 5054-5071.
- 46  
47  
48  
49 36. BGS; DPHE *Arsenic contamination of groundwater in Bangladesh*; D. G. Kinniburgh, P. L.  
50  
51 Smedley, Eds; BGS: Keyworth, 2001.
- 52  
53  
54  
55 37. Afonso, M.D. and Stumm, W. Reductive Dissolution of Iron(III) (Hydr)oxides by Hydrogen-  
56  
57 Sulfide. *Langmuir* **1992**, *8*, 1671-1675.
- 58  
59  
60

1  
2  
3  
4  
5 38. Poulton, S.W. Sulfide oxidation and iron dissolution kinetics during the reaction of dissolved  
6 sulfide with ferrihydrite. *Chem. Geol.* **2003**, *202*, 79-94.  
7  
8

9  
10 39. Wolthers, M.; Charlet, L.; van Der Linde, P.R.; Rickard, D.; van Der Weijden, C.H. Surface  
11 chemistry of disordered mackinawite (FeS). *Geochim. Cosmochim. Acta* **2005**, *69*, 3469-3481.  
12  
13

14  
15 40. Bruno, J.; Wersin, P.; Stumm, W. On the influence of carbonate in mineral dissolution: II. The  
16 solubility of FeCO<sub>3</sub> (s) at 25°C and 1 atm total pressure. *Geochim. Cosmochim. Acta* **1992**, *56*, 1149-  
17 1155.  
18  
19  
20  
21

22  
23 41. Al-Borno, A. and Tomson, M. The temperature dependence of the solubility product constant of  
24 vivianite. *Geochimica et Cosmochimica Acta* **1994**, *58*, 5373-5378.  
25  
26  
27  
28  
29  
30  
31  
32  
33  
34  
35  
36  
37  
38  
39  
40  
41  
42  
43  
44  
45  
46  
47  
48  
49  
50  
51  
52  
53  
54  
55  
56  
57  
58  
59  
60

**Table 1.** Reactions used in “Iron(III) surface complexation model” and “Iron(II) Kd sorption model”

“Iron(III) surface complexation model”	log K (I=0 M, 25 °C)	Reference
$\text{H}_3\text{AsO}_3^\circ = \text{H}_2\text{AsO}_3^- + \text{H}^+$	-9.22	(21)
$\text{H}_2\text{AsO}_3^- = \text{HAsO}_3^{2-} + \text{H}^+$	-12.11	(21)
$\text{HAsO}_3^{2-} = \text{AsO}_3^{3-} + \text{H}^+$	-13.41	(21)
$\equiv(\text{w})\text{FeOH} + \text{H}^+ = \equiv(\text{w})\text{FeOH}_2^+$	7.29	(22)
$\equiv(\text{w})\text{FeOH} = \equiv(\text{w})\text{FeO}^- + \text{H}^+$	-8.93	(22)
$\equiv(\text{w})\text{FeOH} + \text{AsO}_3^{3-} + 3\text{H}^+ = \equiv(\text{w})\text{FeH}_2\text{AsO}_3 + \text{H}_2\text{O}$	38.76	(20)
$\equiv(\text{w})\text{FeOH} + \text{AsO}_3^{3-} + 2\text{H}^+ = \equiv(\text{w})\text{FeHAsO}_3^- + \text{H}_2\text{O}$	31.87	(20)
$\equiv(\text{w})\text{FeOH} + \text{HS}^- = \equiv(\text{w})\text{FeS}^- + \text{H}_2\text{O}$	5.3	(37)
$\equiv(\text{w})\text{FeOH} + \text{HS}^- + \text{H}^+ = \equiv(\text{w})\text{FeHS} + \text{H}_2\text{O}$	10.82	(37)
“Iron(II) Kd sorption model”	Kd in L/g at pH 7 (7.5)	Reference
$\text{H}_3\text{AsO}_3$ sorption on mackinawite	2 (2)	(17)
$\text{H}_3\text{AsO}_3$ sorption on siderite	0.267 (0.4)	(16)
$\text{H}_3\text{AsO}_3$ sorption on magnetite	0.081 (0.215)	(16)
$\text{H}_3\text{AsO}_3$ sorption on fougurite	0.095 (0.57)	(16)
$\text{H}_3\text{AsO}_3$ sorption on vivianite	0.18 (0.18) <sup>a</sup>	(15)

<sup>a</sup> experimental Kd for As(V) is assumed valid for As(III)

**Table 2.** Biogeochemical reactions included in the “1D generic reactive transport model”

<b>Terminal electron accepting processes (biotic pathways)</b>	<b>[EA]<sub>lim</sub><sup>b</sup></b>	<b>Maximum reduction rate (C(0) oxidation rate<sup>a</sup>) mM/year</b>	<b>Reference</b>
Denitrification $4/5\text{NO}_3^- + 1/2\text{C}_2\text{H}_3\text{O}_2^- + 3/10\text{H}^+ \rightarrow 2/5\text{N}_2 + \text{HCO}_3^- + 1/5\text{H}_2\text{O}$	14 mg/L <sup>b</sup>	8/5 (2 <sup>a</sup> )	see text
Sulfate reduction $1/2\text{SO}_4^{2-} + 1/2\text{C}_2\text{H}_3\text{O}_2^- + 1/2\text{H}^+ \rightarrow 1/2\text{H}_2\text{S} + \text{HCO}_3^-$	0.5 mg/L <sup>b</sup>	1 (2 <sup>a</sup> )	(31)
Iron reduction $4\text{FeOOH} + 1/2\text{C}_2\text{H}_3\text{O}_2^- + 15/2\text{H}^+ \rightarrow \text{HCO}_3^- + 4\text{Fe}^{2+} + 6\text{H}_2\text{O}$	42 mM <sup>b</sup>	“High rate” 8 (2 <sup>a</sup> ) “Low rate” 1.5 (0.375 <sup>a</sup> )	see text
<b>Secondary redox reaction (abiotic pathway)</b>		<b>Kinetic rate mn<sup>-1</sup></b>	
$\text{HS}^- + 5\text{H}^+ + 2\text{FeOOH} \rightarrow \text{S}^\circ + 2\text{Fe}^{2+} + 4\text{H}_2\text{O}$		k=1/40	(38), see SI
<b>Precipitation reactions (non redox)</b>	<b>logK</b>		
Mackinawite + H <sup>+</sup> = Fe <sup>2+</sup> + HS <sup>-</sup>	-2.95		(39)
Siderite + H <sup>+</sup> = Fe <sup>2+</sup> + HCO <sub>3</sub> <sup>-</sup>	-0.47		(40)
Vivianite = 3Fe <sup>2+</sup> + 2PO <sub>4</sub> <sup>3-</sup> + 8H <sub>2</sub> O	-35.77		(41)
Calcite + H <sup>+</sup> = Ca <sup>2+</sup> + HCO <sub>3</sub> <sup>-</sup>	1.85		(19)
<b>Adsorption reactions</b>		<b>Kinetic rate s<sup>-1</sup></b>	
H <sub>3</sub> AsO <sub>3</sub> sorption on mackinawite and siderite	-	k=1/100	see Table 1

<sup>a</sup> C(0) oxidation rate is assumed to be constant along the 1D path for nitrate, sulfate and iron reduction and fixed to 2 mM/year corresponding to 1 mM/year for sulfate reduction (see SI). The “high value” 8 mM/year for iron reduction is tested in the sensitivity analysis (see SI) while the “low value” 1.5 mM/year is the fitted value used in scenario (a)

<sup>b</sup> All the concentration limits for Electron Acceptors [EA]<sub>lim</sub> are fitted values

**FIGURE CAPTIONS**

FIGURE 1. Google Earth satellite image [<http://earth.google.com/>] of the study area (Chakdaha) in West Bengal, India. Symbols indicate the positions of needle-sampler profiles I1-I7 along the Hooghly River transect. Because of the oxidation-reduction (redox) conditions, the data material of this study is restricted to the Wells I7, I6, I5, I3 indicated by the red symbols (see SI).

FIGURE 2. Comparison of the results of the simulated scenario (a) with the porewater profiles of As, Fe, S,  $\text{HCO}_3^-$  and  $\text{NO}_3^-$  from the Well I7 (open square), Well I6 (open delta), Well I5 (open circle), Well I3 (open diamond). S is calculated from the  $\text{SO}_4^{2-}$  determinations by ion chromatography (13). In order to compare all the Wells data with the 1D model, a reference depth Z0 is chosen for each Well (see Table 1SI). The solid lines represent aqueous predictions at the time where aqueous As reached its maximum value in scenario (a) with the “low” iron reduction rate (see Table 2 and main text). The simulated Saturation Indices (SI) of calcite and siderite are deduced from the alkalinities measured by titration. The dotted line is the simulated Kd of As onto siderite.

FIGURE 3. Comparison of the depth distribution of chemical zones and respiration processes in three scenarios (see text for details): in scenario (a), nitrate reduction precedes successive dissimilatory sulfate and Fe reduction; in scenario (b), nitrate reduction precedes sulfate reduction and abiotic Fe reduction by  $\text{HS}^-$ ; in scenario (c), nitrate reduction precedes concomitant dissimilatory Fe and sulfate reduction (see SI). In scenario (a), the dissimilatory Fe(III) reduction rate is fixed to the “low value” of 1.5 mM/year. In the left-hand graphs, S(-II), Fe(II) and As(III) are represented at the time when aqueous As(III) reached its maximum value in each scenario, by the dashed-dotted, dashed and solid lines, respectively. In the right-hand graphs, solid Fe(III), mackinawite, siderite concentrations and Fe(II)/Fe molar ratio are shown at this time with the dotted, dashed-dotted, dashed and solid lines, respectively. The aqueous As and Fe(II)/Fe ratios of Wells I3, I5, I6, I7 are also shown with open square, delta, circle and diamond, respectively. In all scenarios, vivianite is not allowed to precipitate.



1  
2  
3  
4  
5 FIGURE 4. Two possible four-phase systems calculated in “Iron(II) Kd sorption model” at pH 7:  
6  
7 mackinawite represents 1 wt.% Fe, vivianite 6 wt.% Fe (see SI) and the other possible phases are  
8  
9 siderite and magnetite (or fougurite).  
10  
11  
12  
13  
14  
15  
16  
17  
18  
19  
20  
21  
22  
23  
24  
25  
26  
27  
28  
29  
30  
31  
32  
33  
34  
35  
36  
37  
38  
39  
40  
41  
42  
43  
44  
45  
46  
47  
48  
49  
50  
51  
52  
53  
54  
55  
56  
57  
58  
59  
60

1  
2  
3  
4  
5  
6  
7  
8  
9  
10  
11  
12  
13  
14  
15  
16  
17  
18  
19  
20  
21  
22  
23  
24  
25  
26  
27  
28  
29  
30  
31  
32  
33  
34  
35  
36  
37  
38  
39  
40  
41  
42  
43  
44  
45  
46  
47  
48  
49  
50  
51  
52  
53  
54  
55  
56  
57  
58  
59  
60

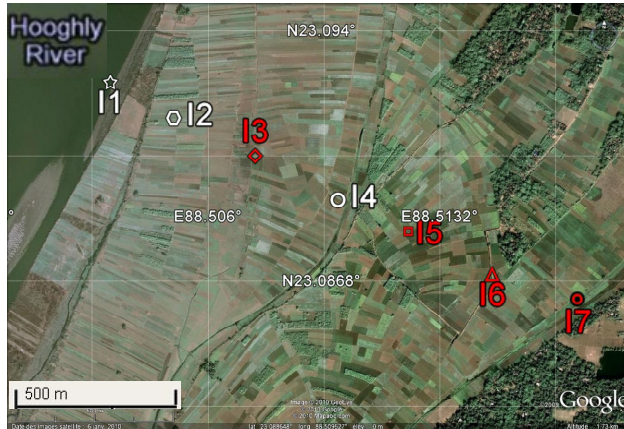


FIGURE 1

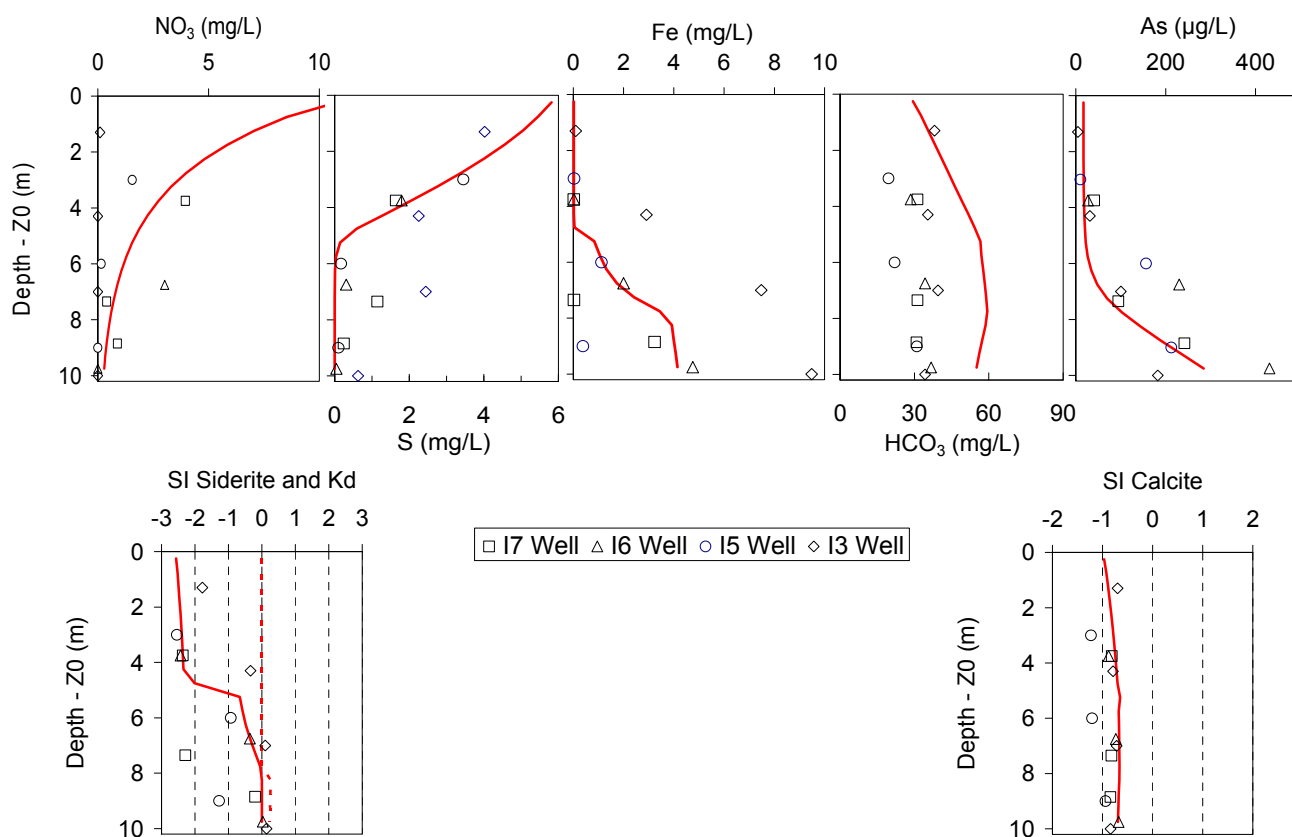


FIGURE 2

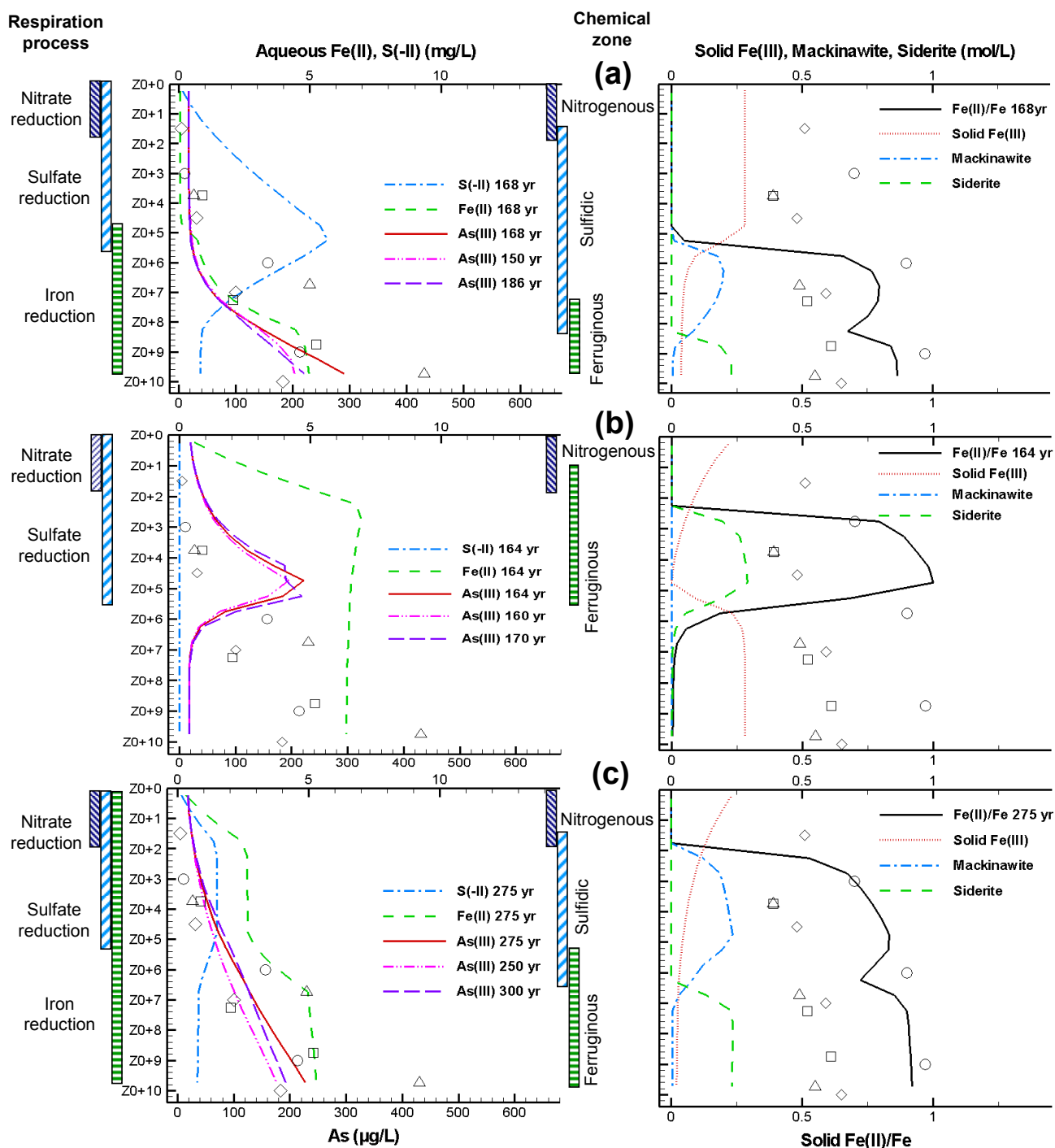


FIGURE 3

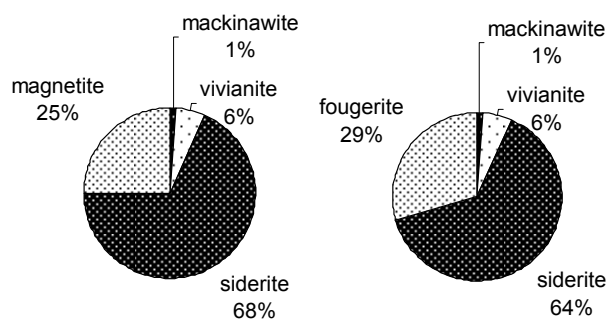


FIGURE 4

1  
2  
3  
4  
5 **Brief:** The nature and distribution of iron-bearing minerals has a prominent impact on arsenic  
6 mobilization in Southeast Asian groundwater  
7  
8  
9  
10  
11  
12  
13  
14  
15  
16  
17  
18  
19  
20  
21  
22  
23  
24  
25  
26  
27  
28  
29  
30  
31  
32  
33  
34  
35  
36  
37  
38  
39  
40  
41  
42  
43  
44  
45  
46  
47  
48  
49  
50  
51  
52  
53  
54  
55  
56  
57  
58  
59  
60